Test Results of Conduction-Cooled Bi-2223 Magnet with Shield Coils at Both Ends

Gen Nishijima and Koji Kamiya

***Abstract*—We have designed and fabricated a superconducting magnet using $(Bi,Pb)_2Sr_2Ba_2Cu_3O_{10}$ (Bi-2223) tape conductors. This magnet is a model magnet for a magnetic refrigeration system for hydrogen liquefaction. The magnet consists of three coils: a main coil and two shield coils. The shield coils generate opposite direction magnetic fields to reduce the magnetic fields to zero at both ends. The Bi-2223 magnet successfully generated a rated field of 4.8 T at the center at 20 K operation. The performance of the magnet at higher operating temperatures was also investigated. The temperature dependence of the performance of this magnet agreed with I_c estimated from the properties of the Bi-2223 tape used at the position of the maximum radial magnetic field in the magnet.**

***Index Terms*—Bi-2223, magnetic refrigeration, superconducting magnet.**

I. Introduction

We have designed and fabricated a superconducting magnet using $(Bi,Pb)_2Sr_2Ba_2Cu_3O_{10}$ (Bi-2223) tape conductors [1]. This magnet is a model magnet to investigate the applicability for a magnetic refrigeration system for hydrogen liquefaction.

The magnetic refrigeration utilizes the magnetocaloric effect. The temperature of the magnetic materials changes in response to changes of the magnetic field. Since a magnetic field of several Tesla is required to obtain the magnetocaloric effect, a superconducting magnet is usually used. Assuming a superconducting solenoid magnet, the magnetic field can be changed by changing the operating current of the magnet or by moving the magnetic material in and out of the bore.

The magnetic refrigeration using the former method, i.e., the magnetic field is changed by changing the operating current, was realized by Park and Jeong using a conduction cooled $GdBa_2Cu_3O_7$ (GdBCO) magnet that generated 3 T in 3 seconds in a 28 mm bore [2]. Hirano et al. also adopts this method to design a magnetic refrigeration system with a $YBa_2Cu_3O_7$ (YBCO) magnet with a 100 mm bore. This magnet is designed to reach 3 T in 2 seconds [3]. The magnetic field changes in high ramp rates cause a temperature rise in the magnet due to AC losses. In addition, controlling the operating current of the magnet at high ramp rates requires a high-voltage power supply that consumes large amount of electric power.

We have demonstrated to liquefy hydrogen by adopting the latter method, i.e., the magnetic material moves in and out of static magnetic field [4]. To achieve the magnetocaloric effect, the magnetic material should experience zero and non-zero magnetic fields. For the magnetic material to experience these magnetic fields by the reciprocation, the magnetic fields at both ends of the magnet should be zero. The NbTi magnet used for this magnetic refrigeration system was equipped with two shield coils. The shield coils, which generate magnetic fields in the opposite direction to that of the main coil, reduce magnetic fields to zero at both ends.

Our goal is to develop high-temperature superconducting (HTS) magnets that could be used in a magnetic refrigeration system for hydrogen liquefaction. In the future, the magnet will be conductively cooled by the hydrogen liquefied by the magnetic refrigeration system itself. We have designed and fabricated the Bi-2223 model magnet to investigate the applicability for the magnetic refrigeration system [1].

In 2022, we tested the magnet at 4 K cooled by a Gifford-McMahon (GM) cryocooler. The test was aborted due to anomalous voltage behavior [1]. We have investigated the cause and made adjustments. After these, we successfully energized the magnet at a rated current at an operating temperature of 20 K. The magnet performance at higher temperatures were also investigated. This paper reports these test results.

II. Bi-2223 Superconducting Magnet

The Bi-2223 superconducting magnet was designed to be compatible with the NbTi magnet used for the magnetic refrigeration system that demonstrated hydrogen liquefaction [4]. The bore size and the height of the magnet are 120 mm and 360 mm, respectively. As already mentioned, the magnet consists of a main coil and two shield coils. The magnetic field at the center was designed to be 4.8 T at an operating current of 300 A. The Detail parameters of the magnet are shown in Table I [1].

The main coil and each shield coil consist of 16 and 4 double pancakes (DPs), respectively. DPs were made of Cu-alloy reinforced Bi-2223 tape conductors (DI-BSCCO Type HT-CA produced by Sumitomo Electric Industries Ltd.). The

Submitted for review October 9, 2023. This work was supported by JST-Mirai Program Grant Number JPMJMI18A3, Japan. *(Corresponding author: Gen Nishijima.)*

G. Nishijima and K. Kamiya are with National Institute for Materials Science (NIMS), Tsukuba, 305-0003 Japan (e-mail: nishijima.gen@nims.go.jp).

Color versions of one or more of the figures in this article are available online at http://ieeexplore.ieee.org

TABLE I
SPECIFICATIONS OF BI2223 SUPERCONDUCTING MAGNET

	Main coil (16DP)	Shield coil (4DP×2)
Inner diameter [mm]	142	150
Outer diameter [mm]	238	226
Height [mm]	166	41
Number of turns	3,592 (224.5/DP)	714×2 (178.5/DP)
Conductor length [m]	2,122 (132.6/DP)	418.4×2 (104.6/DP)
Operating current (I_{op}) [A]	300	
Field contribution at the center [T]	5.43	−0.624
Central magnetic field (B_0) [T]	4.80	
Self inductance [H]	1.45	0.11
Total inductance [H]	1.26	
Stored energy [kJ]	56.7	
Expected I_c at 20 K [A]	359	

conductors were insulated with polyimide tape wrappings. Each DP was epoxy impregnated. A 0.5 mm thick aluminum sheet (hereafter referred to as the cooling sheet) was inserted between the DPs to facilitate heat exchange in the magnet. A photograph of the magnet after assembling the main structure for conduction cooling is shown in Fig. 1. The cooling sheets were connected to two vertical cooling plates. The two plates that sandwich the magnet from above and below are also cooling structures. The two vertical plates and the upper and lower plates were thermally connected to the second stage of the GM cryocooler. The rated cooling capacity of this cryocooler is 1 W at 4 K. To control the magnet temperature above 4 K, heaters were embedded in the second stage of the cryocooler and the two vertical cooling plates.

The magnet was installed in a vacuum chamber specially fabricated for testing. This vacuum chamber has a 90 mm diameter room temperature bore to measure magnetic field profile. The magnet was cooled down to 4 K in 82 hours. A 300 A/± 5 V power supply manufactured by Kudo Electric Co., Ltd. was used to energize the magnet.

III. TEST RESULTS AND DISCUSSION

A. Power Supply Adjustment and 4 K Operation

During the first test campaign in 2022, we were plagued by voltage oscillations at operation currents (I_{op}) above ~200 A

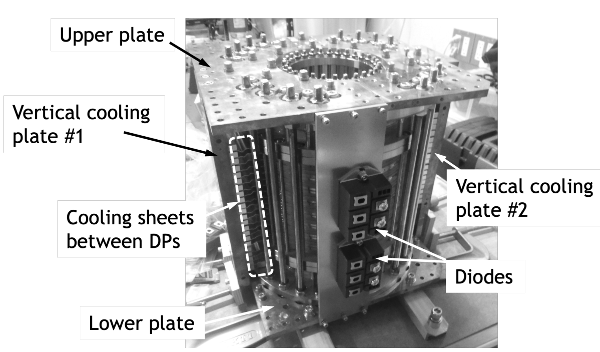

Fig. 1. Photograph of the Bi-2223 magnet after assembling the main structure for conduction cooling.

[1]. As shown in Fig. 2(a), the amplitude of the voltage oscillation increased with increasing I_{op}. Finally, the power supply was shut down at 229 A (B_0 = 3.6 T). After this incident, we inspected the magnet thoroughly and found nothing unusual.

We analyzed stresses applied to the coils due to the magnetic repulsive force between the main coil and the shield coils. The magnetic repulsive force was calculated to be 130 kN at I_{op} = 300 A. The coils are subjected to compressive stresses caused by this magnetic repulsive force. The maximum value of compressive stress was observed at the equatorial plane of the main coil, i.e., z = 0, with a value of –18.6 MPa. On this plane, compressive stresses were distributed radially from –18.6 MPa (inside) to –9.26 MPa (outside). Note that these values were calculated with I_{op} = 300 A and should be much smaller with I_{op} = 229 A. The values were sufficiently smaller than those tested by Wolla *et al.* on an epoxy-impregnated single-pancake coil made of a bare Bi-2223 tape [5]. Since our DPs were made of Bi-2223 tapes reinforced with Cu alloy, they should not be degraded by such small stresses.

Detailed investigation of the voltage oscillation revealed that the oscillation frequency was 10 Hz and that the power supply was a source of the oscillation. A 10 Ω resistor was added between current output terminals of the power supply to be in parallel with the magnet. This adjustment of the power supply eliminated oscillations in the magnet voltage and allowed to be energized up to the rated current of 300 A, which was shown in Fig. 2(b).

Fig. 3(a) shows the time variation of temperatures of the magnet when I_{op} was held at 300 A for 5 hours at an initial temperature of ~4 K (hereafter, T_{ini} ~ 4 K). While During I_{op} increased at 0.2 A/s, the magnet temperatures increased from ~4 K to 7.3–7.7 K due to AC losses. As I_{op} reached 300 A and held, the temperatures decreased about 1 K. The cold end of the HTS current lead (CL) showed the highest temperature, which may be due to the large heat load from the hot end (~40 K). The heat from the copper busbar between the current

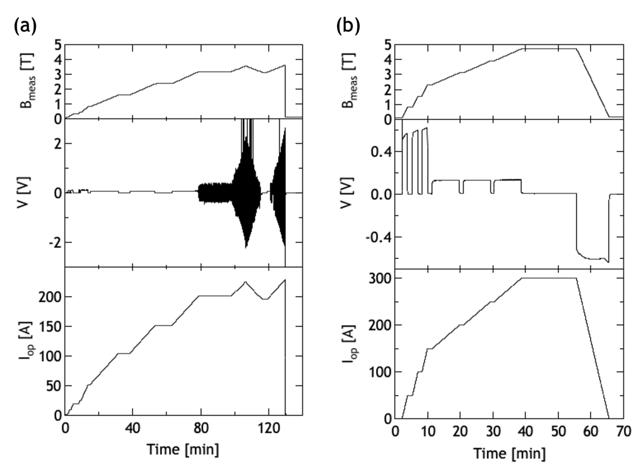

Fig. 2. Magnet voltages (a) observed during excitation test at 4 K in 2022 [1] and (b) observed at 4 K after the power supply adjustment. Voltage oscillations were eliminated.

feedthrough and the HTS CL hot end presumably increased the temperature of the HTS CL hot end and the radiation shield. The busbars should have been optimized by the method described in [6]. However, the results imply that more care should be taken in the design and fabrication of high-current busbars. The heat may also have penetrated through the HTS CL, which increased the temperature of the HTS CL cold end.

B. 20 K Operation

To estimate the performance of the magnet at temperatures above 4 K, critical current (I_c) of the tape used for the DP at the top of the main coil was measured as a function of magnetic field (B) and temperature (T). The DP at the top of the main coil includes the position where the radial magnetic field (B_r), i.e., the magnetic field perpendicular to the tape ($B_\perp$), is maximum. Note that since this magnet is equipped with the shield coils, the radial component of the magnetic field, i.e., the magnetic field perpendicular to the tape, is enhanced at the top and bottom ends of the main coil. Therefore, the Bi-2223

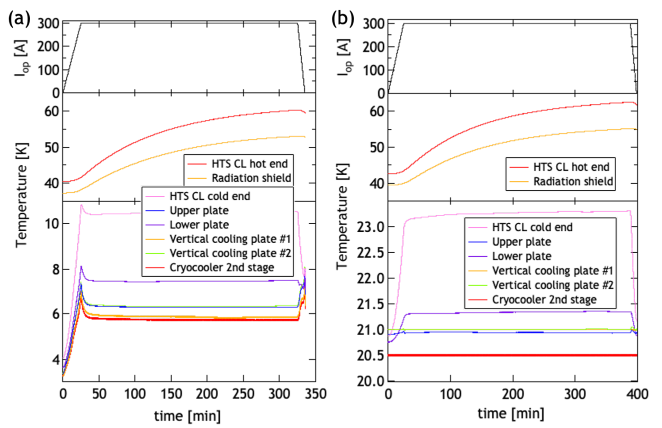

Fig. 3. Time variation of temperatures of the magnet at initial temperatures (T_{ini}) of (a) ~4 K and (b) ~20 K. Although temperatures of the hot end of HTS CL and radiation shield increased about 20 K, the rated magnet field was held for 6 h.

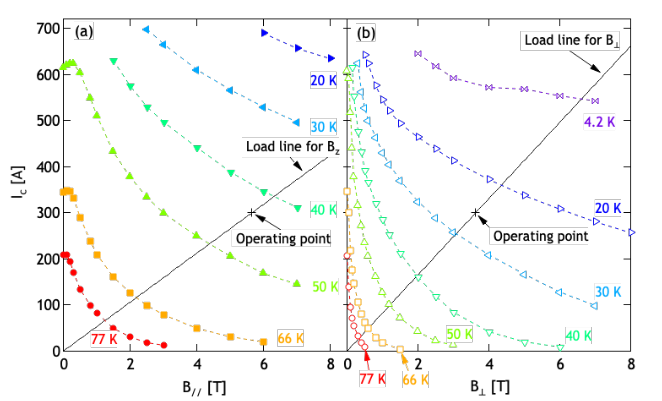

Fig. 4. I_c, determined by 100 μV/m criteria, as a function of magnetic field (B) and temperature (T) for (a) B parallel to tape surface ($B_{//}$) and (b) B perpendicular to tape surface ($B_\perp$) of Bi-2223 tape used for DP at the top of the main coil. Load lines for B_z and B_r are also shown.

tapes, which showed the highest I_c at 77 K in self field among the procured tapes, were used for this DP and the DP the bottom of the main coil [1].

The measured I_c–B at 77, 66, 50, 40, 20, and 4.2 K are shown in Fig. 4. I_c were determined by the electric field criteria of 100 μV/m (1 μV/cm). Load lines calculated for B_z and B_r are also shown. From an intersection between the load line and I_c–$B_\perp$ at 20 K, we can estimate the magnet I_c. The value was estimated to be 359 A at 20 K, indicating a margin of 59 A for the rated current of the magnet (300 A).

The temperature of the magnet was controlled in the range of 20–21 K using heaters embedded in the second stage of the GM cryocooler and the two vertical cooling plates. Fig. 3(b) shows the time variation of temperatures of the magnet when I_{op} was held at 300 A for 6 hours at T_{ini} ~ 20 K. Temperature increase similar to those observed for the operation at T_{ini} ~ 4 K was observed, which should be suppressed by reducing heat loads from the Cu busbars. However, the success of the long-time operation at T_{ini} ~ 20 K will make the next step, i.e., the magnetic refrigeration experiments using this Bi-2223 magnet, possible.

Fig. 5 shows magnetic field profile on the central axis at I_{op} = 300 A at T_{ini} ~ 20 K. The measured profile well agreed the calculated one, indicating the design validity.

C. Effect of Screening Current

As observed in many HTS magnets [7], [8], the effect of the screening current induced magnetic field was observed in this magnet. Fig. 6(a) compares the central magnetic fields measured at T_{ini} ~ 4 K and 20 K (B_{meas}) with the calculated value (B_{cal}). B_{meas} were not zero at I_{op} = 0 because of the residual magnetic field. Hysteresis was also observed. At I_{op} = 300 A, B_{meas} drifted to higher values with time as shown in the inset. After 6-hour holding, B_{meas} was 4.79 T at 20 K. The difference from the calculated value is small, about 10 mT, and probably does not affect magnetic refrigeration.

Fig. 6(b) compares B_{cal}–B_{meas} corresponding to the screening current induced magnetic field obtained at T_{ini} ~ 4 K and 20 K. The higher the operating temperature, the smaller the effect of the screening current. This is because the higher the temperature, the lower the critical current and the smaller the screening current. This is evident from the time variation

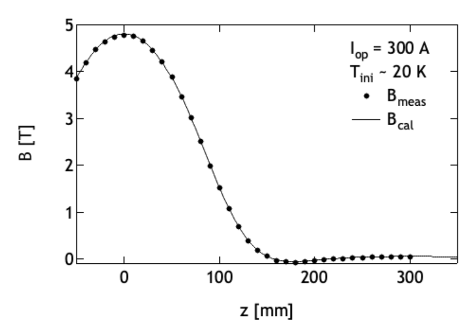

Fig. 5. Measured and calculated magnetic field profiles on the central axis at I_{op} = 300 A. The measured profile well agreed with the calculated one.

of B_{meas} while holding I_{op} = 300 A shown in the inset of Fig. 6(a).

D. Temperature Dependence of Coil Performance

The magnet was tested at T_{ini} ~ 30 K, 40 K, 50 K, 66 K, and 77 K to verify the magnet I_c estimated from intersections between the load line and I_c-$B_\perp$-T shown in Fig. 4(b). Fig. 7 shows magnet voltage as a function of I_{op} obtained at 30 K. The current was increased in steps. The voltage was observed at each step, i.e., when the current was held. Voltage generation indicating normal transition was observed at $I_{op} \geq 230$ A. Similar voltage behaviors were observed at other temperatures. Since the total length of the Bi-2223 tapes used in this magnet was approximately 3 km, the magnet I_c were

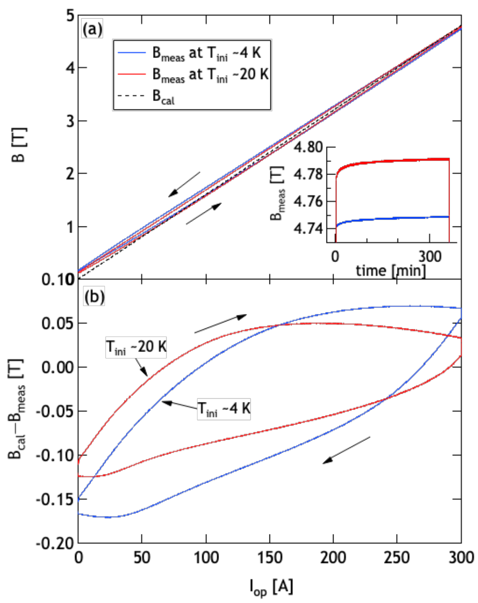

Fig. 6. (a) Measured and calculated central magnetic fields as a function of I_{op}. Inset shows drift of magnetic fields measured at 4 K and 20 K operations. (b) Screening current induced magnetic fields obtained by B_{cal}–B_{meas} as a function of I_{op}. The higher the temperature, the smaller the effect of the screening current induced magnetic field.

determined by voltage criteria of ~ 30 mV, which corresponds to average electric field of 10 μV/m (0.1 μV/cm).

The experimentally evaluated I_c of the magnet at each temperature is shown in Fig. 8. The experimentally obtained I_c agreed with values estimated from I_c-$B_\perp$-T of the tape. For this Bi-2223 magnet, I_c could be estimated by considering the load line for B_r and I_c-$B_\perp$-T of the tape. However, a detailed exploration of the angular dependence of the magnetic field on I_c for DI-BSCCO Type-H reveals that I_c shows its minimum value when the magnetic field is at an angle slightly off from perpendicular to the tape [9]. This implies that in some cases, the magnet I_c is not only determined by the tape I_c at perpendicular magnetic field.

V. Summary

A Bi-2223 superconducting magnet with shield coils at both ends was tested at various temperatures under conduction cooling condition. This magnet was designed and fabricated as a model magnet for a magnetic refrigeration system for hydrogen liquefaction. After an adjustment of the power supply, the magnet successfully generated a rated magnetic field of 4.8 T for 6 hours at an operation current of 300 A at an initial temperature of 20 K. The measured magnetic field profile on the central axis well agreed with the calculated one. The temperature dependence of the magnet performance agrees with the tape I_c obtained from intersections of the of I_c–$B_\perp$–T and the load line.

Although the temperature rise observed while holding the current at 300 A should be suppressed by reducing heat loads from the busbars, the success of the long-time operation will make the next step, the magnetic refrigeration experiments using this Bi-2223 magnet, possible. The interaction between the magnet and the magnetic material moving in and out of its bore should also be investigated [10].

Acknowledgment

The authors would like to thank the staff of Tsukuba Magnet Laboratory, NIMS for supplying liquid helium used to measure critical currents of the Bi-2223 tape.

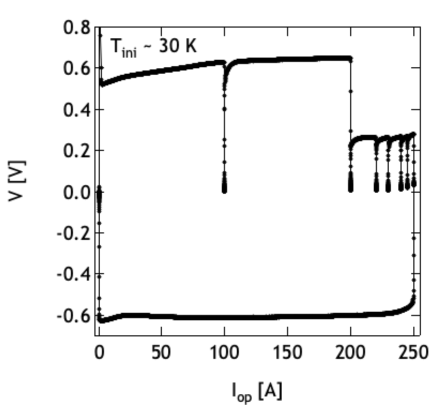

Fig. 7. Magnet voltage as a function of I_{op} measured at 30 K. Voltage generation was observed at $I_{op} \geq 230$ A.

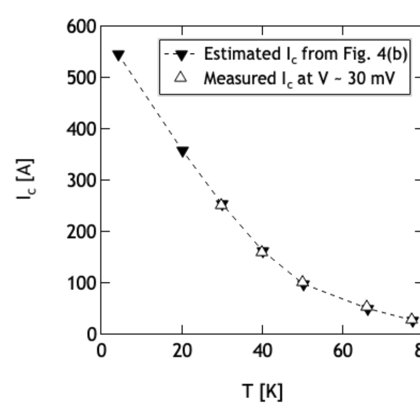

Fig. 8. Comparison of experimentally evaluated I_c of the magnet and estimated values from Fig. 4(b).

References

[1] G. Nishijima, M. Amaya, T. Nishimura, K. Kamiya, and T. Numazawa, "Development of Bi-2223 model magnet for magnetic refrigeration system," *IEEE Trans. Appl. Supercond.,* vol. 33, no. 5, Aug. 2023, doi: 10.1109/TASC.2023.3265907.

[2] I. Park and S. Jeong, "Development of the active magnetic regenerative refrigerator operating between 77 K and 20 K with the conduction cooled high temperature superconducting magnet," *Cryogenics*, vol. 88, pp. 106-115, Dec. 2017, doi: 10.1016/j.cryogenics.2017.09.008.

[3] N. Hirano, Y. Onodera, T. Mito, Y. Motoki, and A. Kawagoe, "Basic research on a static magnetic refrigeration system for cooling to liquid hydrogen temperature," *IEEE Trans. Appl. Supercond.*, vol. 33, no. 5, Aug. 2022, Art. no. 4702605, doi: 10.1109/TASC.2023.3263786.

[4] K. Kamiya *et al.*, "Active magnetic regenerative refrigeration using superconducting solenoid for hydrogen liquefaction," *Appl. Phys. Express*, vol. 15, no. 5, Art. no. 053001, May 2022, doi: 10.35848/1882-0786/ac5723.

[5] J.M. Wolla, R.L. Holtz, and J.P. Voccio, "Axial compression fatigue testing of epoxy impregnated BSCCO coils," *IEEE Trans. Appl. Supercond.* vol. 17, no. 2, pp. 3050-3053, June 2007, doi: 10.1109/TASC.2007.898914.

[6] Y. Iwasa, "Case studies in superconducting magnets," 2nd ed., Springer, 2009, p. 274.

[7] Y. Yanagisawa *et al.*, "Operation of a 500 MHz high temperature superconducting NMR: Towards an NMR spectrometer operating beyond 1 GHz," *J. Magn. Reson.* vol. 203, pp. 274-282, Jan. 2010, doi: 10.1016/j.jmr.2010.01.007.

[8] S. Awaji *et al.*, "First performance test of a 25 T cryogen-free superconducting magnet," *Supercond. Sci. Technol*., vol. 30, no. 6, Art. no. 065001, May 2017, doi: 10.1088/1361-6668/aa6676.

[9] S. Wimbush, N. Strickland, and A. Pantoja, "Critical current characterisation of Sumitomo Type H DI-BSCCO® superconducting wire," figshare. Dataset. 2014, doi: 10.6084/m9.figshare.1112565.v9.

[10] K. Natsume *et al.*, "Effects on moving magnetic materials in and out of superconducting magnet for active magnetic regenerative refrigeration system," presented at MT18, Aix-en-Provence, France, 2023.